Int. J. Heat Mass Transfer. Vol. 29, No. 5, pp. 741–751, 1986
Printed in Great Britain

0017–9310/86 $3.00 + 0.00
Pergamon Journals Ltd.

An electrochemical method for determining natural convection mass transfer boundary-layer thicknesses

PETER N. PINTAURO
Department of Chemical Engineering, University of California, Los Angeles, CA 90024, U.S.A.

(*Received* 27 *June* 1985 *and in final form* 25 *November* 1985)

Abstract—A non-contact electrochemical method for determining natural convection mass transfer boundary-layer thicknesses was developed and tested. The transient decay in concentration overpotential after current interruption was matched to a theoretical surface concentration decay model. Boundary-layer thicknesses were determined by equating the real time scale of the experimental data and the dimensionless time scale of the theoretical analysis. The curve-fitting technique was tested by performing a series of overpotential decay experiments at a vertical, flat plate copper cathode immersed in a 0.15 M $CuSO_4$–1.85 M H_2SO_4 solution. The resulting steady-state boundary-layer thicknesses decreased from 0.049 to 0.041 cm as the applied current was increased.

INTRODUCTION

NATURAL convection along an electrode plays an important role in many electrolytic processes by affecting the reaction rate at the electrode surface. For the case of copper deposition or dissolution at a planar, vertical electrode from an unstirred electrolyte, a hydrodynamic flow is generated by density differences between the bulk solution and the electrolyte in the vicinity of the electrode surface. When Cu^{2+} ions are reduced to copper metal at a cathode, the cupric ion concentration in the diffusion layer is decreased, resulting in a less dense solution and an upward hydrodynamic flow. Similarly, during copper dissolution at an anode, the increased concentration of Cu^{2+} at the electrode surface causes the fluid to flow downward.

Previous experimental and theoretical work on this subject can be broadly categorized as: (a) limiting current density analyses [1–3]; (b) solutions of the Von Karman integral equations [3–7]; (c) interferometric measurements of concentration profiles [6–15]; and (d) direct contact experimental methods [16, 17]. In most cases the analyses were performed for copper deposition (reduction) from a $CuSO_4$ or $CuSO_4/H_2SO_4$ supporting electrolyte to a vertical, flat plate electrode.

Much of the early experimental research focused on investigating the limiting current deposition of copper. At the limiting current, the electrode surface concentration of Cu^{2+} is virtually zero and the reduction rate for cupric ions is a maximum. From these experiments, a Sherwood–Schmidt–Grashof number correlation, analogous to that for natural convection heat transfer, was developed [1]

$$\overline{Sh} = 0.677(Sc\ \overline{Gr})^{1/4}. \quad (1)$$

Selman and Newman [2] performed a theoretical analysis of steady-state natural convection mass transfer at the limiting current. Computer simulations revealed the effect of supporting electrolyte on the concentration, velocity and solution density profiles.

The Von Karman–Pohlhausen integral method has been used to model natural convection mass transfer below the limiting current. Ibl and Braun [4] found that the mass transfer boundary-layer thickness at a cathode varied directly as the 1/5 power of the electrode height and inversely as the 1/5 power of the applied current. These results were recently confirmed by the theoretical and interferometric studies of Awakura *et al.* [7], Fukunaka *et al.* [11] and Denpo *et al.* [12]. The latter developed the following correlation equation for natural convection copper deposition from a $CuSO_4/H_2SO_4$ electrolyte:

$$Sh = 0.628(Sc\ Gr^*)^{1/5}. \quad (2)$$

Fukunaka and co-workers also used interferometry to examine the transient behavior of natural convection $CuSO_4$ concentration profiles adjacent to a vertical copper electrode when current is applied, interrupted and reversed [13–15].

Direct contact experimental methods for measuring natural convection mass transfer boundary-layer thicknesses have also been examined, with limited success. Brenner's freezing technique [16] and the direct sampling method developed by Read and Graham [17] were found to be time consuming and gave only a qualitative description of concentration changes near the electrode surface.

The analysis presented in this paper examines a non-contact method of measuring natural convection mass transfer boundary-layer thicknesses at a vertical, flat plate electrode. The method converts a transient decay of concentration overpotential after steady-state current interruption to a dimensionless concentration

NOMENCLATURE

- C concentration of reacting species [mol cm^{-3}]
- D diffusion coefficient of reacting species [cm^2 s^{-1}]
- $\mathscr{F}$ Faraday's constant, 96,487 Coulombs g-equiv^{-1}
- F dimensionless streamfunction defined by equation (19)
- g gravitational acceleration, 980 cm^2 s^{-1}
- $\overline{Gr}$ average grashof number over electrode of height L, $g\Delta\rho L^3/\rho_\infty \nu^2$, dimensionless
- Gr^* modified Grashof number, $g\alpha i(1-\Gamma_1)x^4/z\mathscr{F}\nu^2 D$, dimensionless
- i current density [A cm^{-2}]
- i_L limiting current density [A cm^{-2}]
- L electrode height [cm]
- n number of electrons involved in the electrode reaction [g-equiv mol^{-1}]
- R gas constant, 8.314 J gmol^{-1} K^{-1}
- Sc Schmidt number, ν/D, dimensionless
- Sh Sherwood number, x/δ, dimensionless
- $\overline{Sh}$ average Sherwood number, over electrode of height L, L/δ, dimensionless
- T temperature [K]
- t time [s]
- u velocity parallel to the electrode [cm s^{-1}]
- v velocity perpendicular to the electrode [cm s^{-1}]
- x vertical distance along the electrode measured from the leading edge of the boundary layer [cm]
- Y dimensionless perpendicular distance, defined by equation (9)
- y distance perpendicular to the electrode surface [cm]
- Z Ionic charge, positive for cations, negative for anions [g-equiv mol^{-1}].

Greek symbols

- α densification coefficient [cm^3 mol^{-1}]
- δ mass transfer boundary-layer thickness [cm]
- $\bar{\delta}$ average value of δ in the vertical direction [cm]
- δ_{eff} effective mass transfer boundary-layer thickness [cm]
- ε electrode potential [V]
- ε^r equilibrium reversible electrode potential [V]
- ξ similarity variable representing dimensionless distance, defined by equation (18)
- Γ transference number, dimensionless
- ν kinematic viscosity [cm^2 s^{-1}]
- η concentration overpotential [V]
- $\bar{\eta}$ average concentration overpotential, as measured over the entire electrode surface [V]
- Φ dimensionless concentration, defined by equation (4)
- $\bar{\Phi}$ average value of Φ in the vertical direction.
- ψ streamfunction [cm^2 s^{-1}]
- ρ density [g cm^{-3}]
- $\Delta\rho$ $= \rho_\infty - \rho_s$[g cm^{-3}]
- τ dimensionless time, defined by equation (8)
- $\hat{\tau}$ dimensionless time, defined by equation (20).

Subscripts

- 1 Cu^{2+}
- 2 H^+
- 3 SO_4^{2-}
- ∞ bulk solution
- s electrode surface.
- 0 Initial time.

fraction. Mass transfer boundary-layer thicknesses are calculated by matching the experimental data to a theoretically determined, surface concentration decay curve which is a function of time, the steady-state boundary-layer thickness and the diffusion coefficient. The principal advantages of this method over other techniques for determining boundary-layer thicknesses are: (a) it does not require an elaborate and expensive experimental apparatus; (b) it is applicable at currents less than the limiting current; and (c) it can be used to analyze mass transfer at either an anode or a cathode.

Nanis originally proposed this technique for measuring the thickness of mass transfer boundary layers at a dissolving metal anode with natural convection stirring [18]. The time-dependent decay in excess surface concentration after current interruption was modeled by analyzing two extreme cases which bounded the actual collapse of the mass transfer boundary layer: mass transfer by pure diffusion and mass transfer with perfect stirring. The simple mathematical analysis of Nanis, however, assumed that the concentration profiles in the mass transfer boundary layer were linear and his perfect stirring model lacked a clearly defined physical basis because it did not directly take into account convective flows adjacent to the electrode surface. In the present study, a more thorough theoretical analysis of concentration changes at an electrode surface in the absence and presence of natural convection fluid flows has been performed. The theoretical analysis has been tested by

carrying out a series of overpotential decay experiments at a vertical, flat plate copper cathode immersed in a $CuSO_4$–H_2SO_4 solution.

THEORETICAL

In electrochemical systems, the steady-state concentration profile of reacting species in the mass transfer boundary layer is maintained constant, until the applied current is interrupted. When the current flow stops, the concentration in the boundary layer returns to the bulk solution concentration and the electrode potential (ε) returns to the rest potential (ε^r) in accordance with the Nernst equation. The difference in ε and ε^r is known as the concentration overpotential (η). For an ideal solution and a single electrode reaction involving a single reacting species, η is given by

$$\eta = \varepsilon - \varepsilon^r = \frac{RT}{n\mathscr{F}} \ln \frac{c(x, 0, t)}{c(x, \infty, t)}. \tag{3}$$

$c(x, y, t)$, the concentration of reacting species, is a function of the time after current interruption (t) and the distances parallel (x) and perpendicular (y) to the electrode surface. When the Nernst equation is combined with a dimensionless concentration fraction (Φ) defined as

$$\Phi = \frac{c(x, y, t) - c(x, \infty, t)}{c(x, y, 0) - c(x, \infty, t)}, \tag{4}$$

a concentration overpotential/electrode surface concentration fraction relationship is found, which for a cathodic reaction, is

$$\Phi_s = \frac{1 - \exp[-n|\eta|\mathscr{F}/RT]}{1 - \exp[-n|\eta_0|\mathscr{F}/RT]}. \tag{5}$$

For an anodic reaction, Φ_s is given by

$$\Phi_s = \frac{\exp[n\eta\mathscr{F}/RT] - 1}{\exp[n\eta_0\mathscr{F}/RT] - 1}. \tag{6}$$

In equations (5) and (6), Φ_s is the value of Φ at the electrode surface ($y = 0$) and η_0 is the concentration overpotential at current interruption ($t = 0$). These two equations can be used to relate experimentally measured concentration overpotentials after current interruption to a theoretical model of transient concentration changes at an electrode surface.

The mathematical analysis of transient natural convection mass transfer is highly complex because of coupling between the changing hydrodynamic flows and concentration gradients. To simplify the analysis, concentration changes near the electrode surface after current interruption were modeled by examining two limiting cases which uncouple fluid flow and mass transfer: (a) transient concentration changes by simple diffusion (slow decay); and (b) transient decay by convective diffusion with constant fluid velocities parallel and perpendicular to the electrode surface (fast decay). Intermediate to these two extreme conditions must lie the 'mixed' controlled collapse of the boundary layer by both natural convection stirring and diffusion.

Slow decay

The slowest possible decay of the concentration differences in the mass transfer boundary layer (δ) would occur if all the convective flows were reduced to zero at the instant of current interruption. For this simple diffusion extreme Fick's second law was solved,

$$\frac{\partial \Phi}{\partial \tau} = \frac{\partial^2 \Phi}{\partial Y^2} \tag{7}$$

where τ and Y are the dimensionless time and distance, given by

$$\tau = Dt/\delta^2 \tag{8}$$

$$Y = y/\delta. \tag{9}$$

The initial condition for equation (7) is the steady-state concentration profile prior to current interruption. This profile has been determined experimentally for a $Cu/CuSO_4$–H_2SO_4 system [12] and can be described by the Von Karman–Pohlhausen approximation [3],

$$\Phi = (1 - Y)^2. \tag{10}$$

The boundary conditions for this problem are:

$$\text{at} \quad Y = 0 \quad \frac{\partial \Phi}{\partial Y} = 0 \tag{11}$$

$$\text{as} \quad Y \to \infty \quad \Phi = 0. \tag{12}$$

Equation (7) was solved, subject to conditions (10)–(12), by the Laplace transform method. The transient decay in the surface concentration Φ_s is given by [19]

$$\Phi_s = [1 - 2\tau] \operatorname{erf} \frac{1}{2(\tau)^{1/2}} + 2(\tau/\pi)^{1/2}[\exp(-1/4\tau) - 2]. \tag{13}$$

From the properties of the error function and the descending exponential, equation (13) can be approximated over certain ranges of τ by the following simple relationships:

$$\Phi_s = 1 + 2\tau - 4(\tau/\pi)^{1/2} \quad 0 < \tau \leqslant 0.1 \tag{14}$$

$$\Phi_s = \frac{1}{3(\pi\tau)^{1/2}} \quad 3.0 \leqslant \tau < \infty. \tag{15}$$

Fast decay

In the analysis presented by Nanis for his perfect stirring fast decay extreme [18], the transient diffusion equation [equation (7)] was solved for the case of a constant mass transfer boundary-layer thickness—i.e. the boundary condition given by equation (12) was replaced by $\Phi = 0$ at $Y = 1$. In the analysis presented below, fluid flows are directly included in the fast decay model by solving the transient convective mass transfer equation with electrolyte velocities parallel and perpendicular to the electrode surface.

From a theoretical viewpoint, the fastest decay of the electrode surface concentration after current interruption would occur if the steady-state convective flows were to continue without diminishing until the concentration differences between the bulk and boundary-layer solutions were zero. The assumption of

constant velocities parallel and perpendicular to the electrode uncouples the hydrodynamic and mass transfer equations. In addition, the highest steady-state, natural convection velocities would occur at the limiting current, when the cathode surface concentration of reacting species is virtually zero and the density gradients are at a maximum. Thus, for the fast decay model, the convective mass transfer equation was solved with constant, limiting current velocities parallel and perpendicular to the electrode.

The transient, two-dimensional, convective mass transfer equation which describes concentration changes near a vertical flat plate electrode after current interruption is:

$$\frac{\partial \Phi}{\partial t} + u\frac{\partial \Phi}{\partial x} + v\frac{\partial \Phi}{\partial y} = D\frac{\partial^2 \Phi}{\partial x^2} \tag{16}$$

where u and v are the velocities parallel and perpendicular to the electrode, respectively. By introducing a similarity variable for dimensionless distance (ξ), a dimensionless streamfunction $F(\xi)$ and a dimensionless time ($\hat{\tau}$), equation (16) becomes

$$\frac{\partial \Phi}{\partial \hat{\tau}} = \frac{A^2\delta^2}{L^{1/2}} F(\xi)\frac{\partial \Phi}{\partial \xi} + \frac{A^2\delta^2}{L^{1/2}}\frac{\partial^2 \Phi}{\partial \xi^2} \tag{17}$$

where

$$\xi = \frac{Ay}{x^{1/4}} \tag{18}$$

$$F(\xi) = \frac{3\psi}{4DxA} \tag{19}$$

$$\hat{\tau} = \frac{Dt}{\delta^2}\left(\frac{L}{x}\right)^{1/2} = \tau\left(\frac{L}{x}\right)^{1/2} \tag{20}$$

and

$$A = \left(\frac{3g}{4\nu D}\frac{\Delta\rho}{\rho_\infty}\right)^{1/4}. \tag{21}$$

In the above equations L is the electrode height, g is the gravitational acceleration, $\Delta\rho/\rho_\infty$ is the normalized average density difference in the boundary layer and ψ is the streamfunction, defined so that the equation of continuity is satisfied, i.e.

$$u = \frac{\partial \psi}{\partial y}, \quad v = -\frac{\partial \psi}{\partial x}. \tag{22}$$

The boundary and initial conditions for the fast decay are identical to those for the slow decay analysis and, in terms of ξ, are given by:

$$t > 0 \quad \text{at} \quad \xi = 0 \quad \frac{\partial \Phi}{\partial \xi} = 0 \tag{23}$$

$$\text{as} \quad \xi \to \infty \quad \Phi = 0 \tag{24}$$

$$\text{at} \quad t = 0 \quad \Phi = \left(1 - \frac{\xi x^{1/4}}{A\delta}\right)^2. \tag{25}$$

A computer solution to equation (17) was obtained using a finite-difference numerical method. A time-independent $F(\xi)$ distribution, determined from the steady-state, limiting current theoretical analysis of Selman and Newman ([2, Fig. 2] for complete dissociation of H_2SO_4 into H^+ and SO_4^{2-}) was inserted into equation (17). The analysis was carried out for an electrode of height 9.2 cm, immersed in a 0.15 M $CuSO_4$–1.85 M H_2SO_4 electrolytic solution. The physical constants used in the determination of the constant A [equation (21)] were estimated from data in the literature and are listed in Table 1.

The slow and fast decay models for the transient surface concentration decay are compared on the same Φ_s vs log τ plot by converting the computed Φ_s vs $\hat{\tau}$ results to Φ_s vs τ—i.e. multiply $\hat{\tau}$ by $(x/L)^{1/2}$. Figure 1, for $x/L = \frac{1}{2}$, shows that the slow decay [equation (13)] and fast decay extremes coincide exactly for $1.0 > \Phi_s > 0.78$. Thus, for small τ the time behavior of the concentration at the electrode surface is independent of fluid flow conditions and the theoretical decay can be described by the simple analytical relationship given by equation (14). Although the boundary-layer thickness appears in the initial condition [equation (25)] and the coefficients of the derivative terms in equation (17), the initial stages of the surface concentration decay are also independent of δ.

To determine the mass transfer boundary-layer thickness at the vertical midpoint of a flat plate cathode, concentration overpotentials after current interruption (measured at $x/L = \frac{1}{2}$) are converted to Φ_s vs time data and fitted to the single theoretical Φ_s vs log τ curve for $\tau < 0.01$. The real and dimensionless time scales are then equated and the boundary-layer thickness is determined from

$$\delta = \left(\frac{Dt}{\tau}\right)^{1/2}. \tag{26}$$

In the fast decay model, the vertical distance from the leading edge of the boundary layer (x) appears in the initial condition and the dimensionless time variable, $\hat{\tau}$. By changing the value of x in the fast decay computer program, Φ_s vs log τ curves were obtained for different vertical heights along the electrode. Fast decay curves for $\delta = 0.06$ cm and $x/L = 0.3$ and 0.6 are compared to the slow decay extreme in Fig. 2. When $\tau < 0.013$, the concentration decay is independent of x, while for $\tau > 0.013$, Φ_s is a weak function of vertical distance [through the x dependence in equation (25)]. The

Table 1. Physical property data for a 0.15 M $CuSO_4$–1.85 M H_2SO_4 electrolytic solution at 25°C

D	5.13×10^{-6} cm^2 s^{-1} [20]
ν	1.18×10^{-2} cm^2 s^{-1} [21]
α_1	140 cm^3 mol^{-1} [2]
α_2	29.9 cm^3 mole^{-1} [2]
$\Delta\rho/\rho_\infty$	8.45×10^{-3} [2, 10]
Z_1	+2 g-equiv mol
Z_2	+1 g-equiv mol^{-1}
Z_3	−2 g-equiv mol^{-1}
Γ_1	0.01 [11, 21]
Γ_2	0.81 [11]

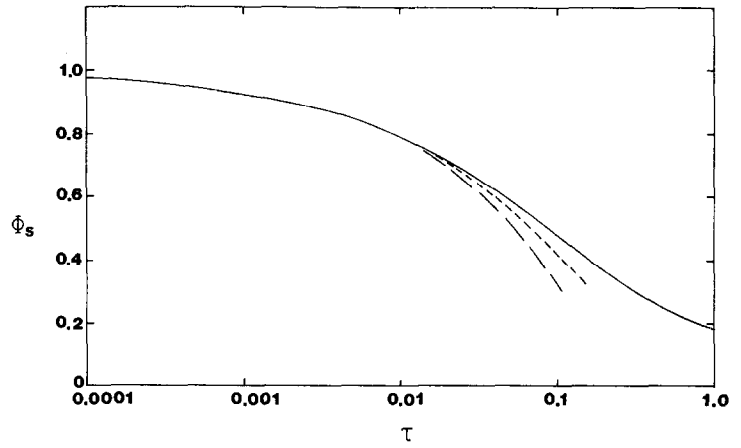

FIG. 1. Comparison of the slow and fast decay models. —— slow decay, equation (13); — — — fast decay (with $x/L = \frac{1}{2}$ and $\delta = 0.04$ cm); - - - - - fast decay (with $x/L = \frac{1}{2}$ and $\delta = 0.06$ cm).

analysis predicts that the boundary layer will collapse faster as its leading edge is approached.

Decay curves similar to those shown in Fig. 1 and 2 can be used to analyze the transient decay of the local concentration overpotential at any height along the electrode surface. When average concentration overpotentials (as measured over the entire electrode surface) are recorded in an experiment, the $\bar{\eta}$ vs t data must be matched to the theoretical decay of a height-averaged surface concentration ($\bar{\Phi}_s$). The slow decay analysis discussed above was independent of vertical distance, hence Φ_s, given by equation (13), is equal to $\bar{\Phi}_s$. For the fast decay case $\bar{\Phi}_s$ is obtained, for a given value of τ, by integrating Φ_s over an electrode of height L

$$\bar{\Phi}_s(\tau) = \frac{1}{L}\int_0^L \Phi_s(x, \tau)\, dx. \qquad (27)$$

The integration in equation (27) was performed numerically and the resulting fast decay curve is compared to the slow decay extreme in Fig. 3. As in Figs. 1 and 2, the transient decay of $\bar{\Phi}_s$ for small τ is independent of the presence or absence of fluid motion. The average boundary-layer thickness ($\bar{\delta}$) over an electrode of height L can be determined by matching experimental overpotential data to this theoretical model.

EXPERIMENTAL

In order to test the theoretical decay model for determining mass transfer boundary-layer thicknesses, a series of transient cathodic concentration overpotential decay experiments were performed using vertical flat sheet electrodes. In contrast to other experimental methods of determining δ which require highly sophisticated equipment, e.g. interferometry, the curve-fitting technique uses a simple experimental apparatus consisting of an electrolytic cell and auxiliary equipment for measuring current and electrode potentials.

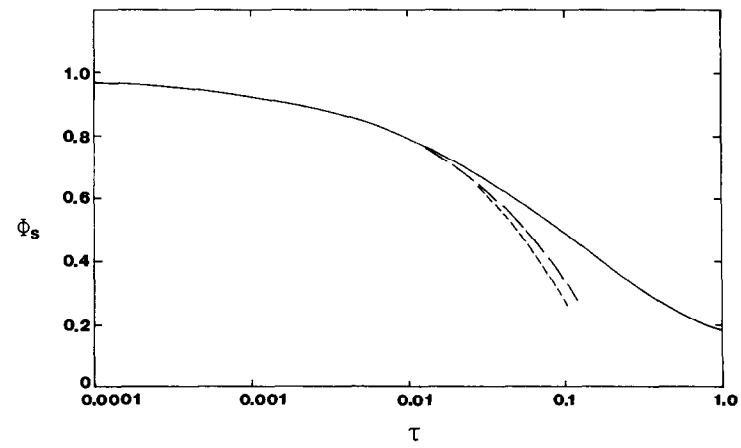

FIG. 2. The fast decay model at two vertical distances away from the leading edge of the boundary layer. —— slow decay, equation (13); — — — fast decay ($\delta = 0.06$ cm and $x/L = 0.6$); - - - - - fast decay ($\delta = 0.06$ cm and $x/L = 0.3$).

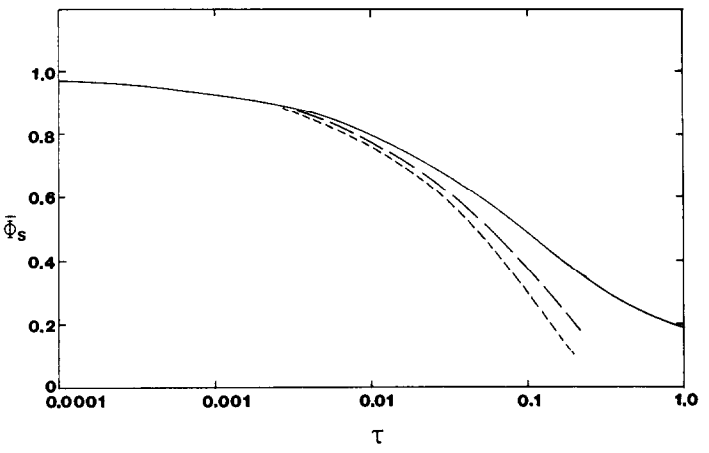

FIG. 3. The theoretical decay of the height-averaged surface concentration fraction. —— slow decay, equation (13); — — — fast decay ($\delta = 0.04$ cm); - - - - - fast decay ($\delta = 0.06$ cm).

The anode and cathode were flat plates of high purity, oxygen -free copper: 25 cm long, 7.0 cm wide and 0.1 cm thick. The backs and sides of the electrodes were insulated with a thin coating of vinyl resin. The electrodes were placed at the far ends of a rectangular Plexiglass tank, 25 cm in length, 7.2 cm in width and 20 cm in height. The container was filled to a depth of 9.2 cm with a 0.15 M $CuSO_4$–1.85 M H_2SO_4 solution. The electrode surface area exposed to electrolyte was 64.4 cm^2. Concentration overpotentials were measured with a remote copper foil reference electrode which contacted the solution in the electrolytic cell via a glass luggin probe. The probe was positioned 3.5 cm above the lower edge of the cathode and 0.2 cm from the electrode surface.

Potentials between the reference electrode and cathode were measured with a Kiethly 168 digital multimeter and the transient overpotential decay was monitored with a Varian model 9176 strip-chart recorder. Direct currents were supplied by a Hewlett-Packard Harrison 6201B power supply, regulated with a decade resistance box and measured with a Simpson ultra high sensitivity microammeter.

Reagent grade chemicals and doubly distilled water were used to prepare the electrolytic solution. The solution temperature for all experiments was 25 ± 1°C.

During a cathodic overpotential decay experiment, a known constant current was applied for ~5 min. After 3 min the cathode potential stabilized, indicating that steady-state had been attained. The current was then interrupted and the subsequent decay in the average overpotential over the entire electrode surface was recorded. Decay experiments were performed for applied currents ranging from 124 to 400 mA. From an independent galvanostatic polarization experiment the limiting current was found to be 407 mA ($i_L = 6.32 \times 10^{-3}$ A cm^{-2}). Most overpotential decay experiments were repeated twice as a check for reproducibility. Typical experimental overpotential vs time data after current interruption are shown in Fig. 4 for $i = 1.93 \times 10^{-3}$ A cm^{-2} and $i = 6.21 \times 10^{-3}$ A cm^{-2}.

RESULTS AND DISCUSSION

Average mass transfer boundary-layer thicknesses, $\bar{\delta}$, over the entire cathode surface were determined from equation (26) (with $D = 5.13 \times 10^{-6}$ cm^2 s^{-1}) by visually matching the concentration overpotential data to the theoretical decay model shown in Fig. 3 (with $\delta = 0.06$ cm). Average concentration overpotentials after current interruption were converted to a dimensionless concentration fraction using equation (5). Values of $\bar{\eta}_0$ needed in the calculation of $\bar{\Phi}_s$, however, could not readily be determined from the recorder traces because they were hidden in the simultaneously decaying resistance and activation overpotentials. The method of superimposing the experimental concentration overpotential data on the theoretical decay curve is based on the reasonable assumption that the resistance and activation overpotentials completely decay $\ll 0.1$ s after current interruption. The pen response time and the maximum chart speed on the recorder used in the experiments were not fast enough to monitor the end of these overpotential decays. Therefore, a trial and error procedure, with different values of $\bar{\eta}_0$, was used with each set of $\bar{\eta}$ vs time data to find that value of $\bar{\eta}_0$ which would permit the transient decay data to: (a) fit the single theoretical decay curve for $\tau < 0.003$; and (b) fall between the slow and fast decay extremes for $\tau > 0.003$.

Representative examples of experimental data (at three different applied currents), which were fitted to the theoretical decay model, are shown in Figs. 5–7. Experimental values of $\bar{\Phi}_s$ for the initial 4 s of the overpotential decay coincide with the slow decay curve. In no experiment did the overpotential fraction, when matched to the theoretical decay for small τ, drop below the fast decay extreme for large τ. As in the theoretical analysis of $\bar{\Phi}_s$ for small τ, the experimental surface concentration decay is independent of fluid motion for short times after current interruption. The experimental data points closely follow the theoretical, simple diffusion extreme for the initial decay period because

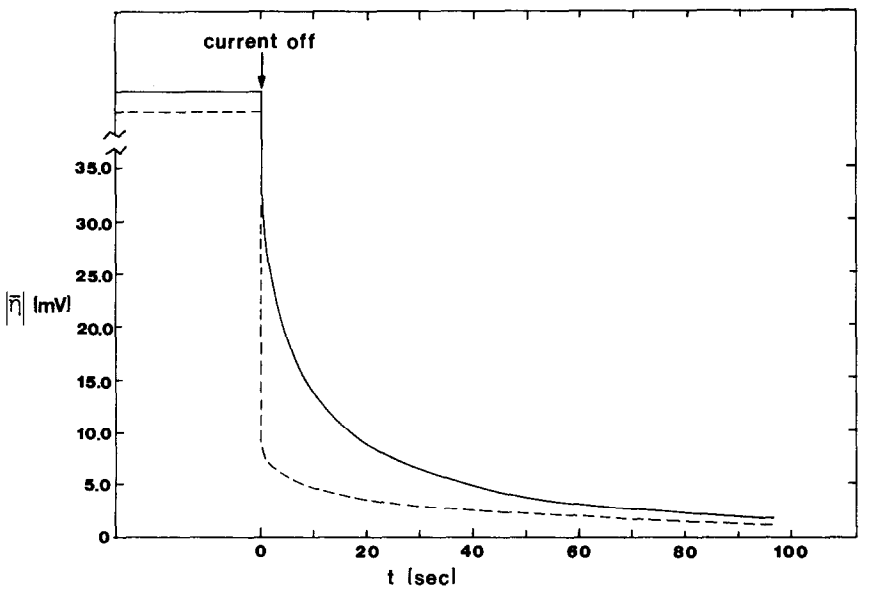

FIG. 4. Experimental overpotential vs time plots after current interruption (0.15 M $CuSO_4$ and 1.85 M H_2SO_4, 9.2 cm electrode height). —— $i = 6.21 \times 10^{-3}$ A cm^{-2} ($i/i_L = 0.983$); – – – – $i = 1.93 \times 10^{-3}$ A cm^{-2} ($i/i_L = 0.305$).

the magnitude of the fluid velocity in the immediate vicinity of the electrode is small [6] and the electrolyte velocity at the electrode surface is zero (the no-slip hydrodynamic condition). A finite period of time (~4 s) is needed for the velocities to transport material from the bulk solution to the electrode surface, hence, diffusion is the primary mode of mass transfer near the electrode surface immediately after current interruption.

Although only two or three experimental data points fall on the single theoretical decay curve for $\tau < 0.003$, the accuracy of the curve-fitting technique of determining δ was not compromised. When the theory and data were matched, a value of real time, t, corresponding to any value of τ could be estimated to within $\pm 5\%$. Since the boundary-layer thickness is proportional to $(t/\tau)^{1/2}$, the resulting values of δ were accurate to within $\pm 2.5\%$. To obtain additional experimental data points in the single decay curve region, concentration overpotentials for $t < 1.0$ s must be collected, suggesting a more sophisticated oscilloscope monitoring technique. This was not attempted in these initial experiments.

Boundary-layer thicknesses calculated from 19 overpotential decay experiments are plotted against the ratio of the applied and limited current densities in

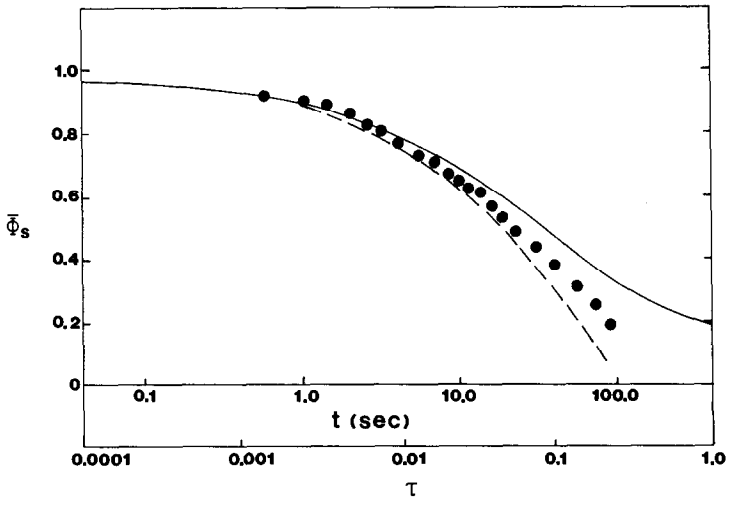

FIG. 5. Decay data from a cathode experiment at $i = 1.93 \times 10^{-3}$ A cm^{-2} ($i/i_L = 0.305$). —— slow decay, equation (13); — — — fast decay ($\delta = 0.06$ cm); ● experimental $\bar{\Phi}_s$.

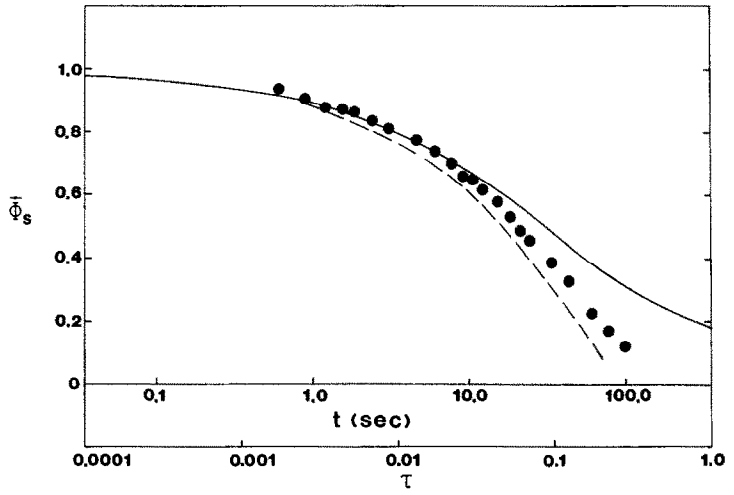

FIG. 6. Decay data from a cathode experiment at $i = 3.73 \times 10^{-3}$ A cm^{-2} ($i/i_L = 0.590$). —— slow decay; — — — fast decay ($\delta = 0.06$ cm); ● experimental $\bar{\Phi}_s$.

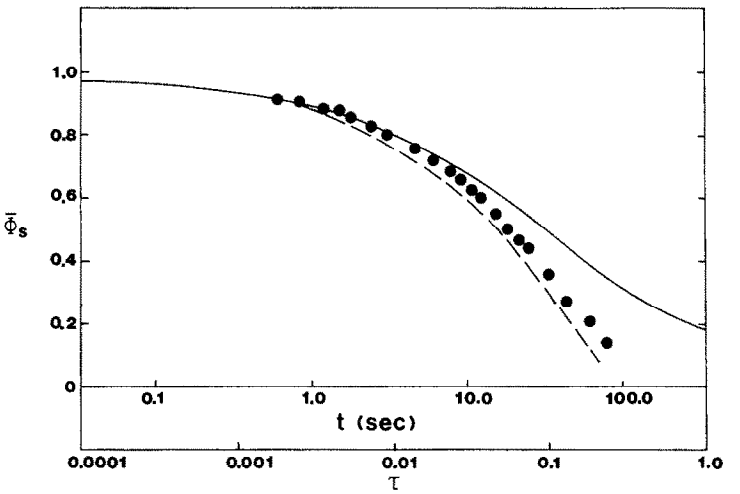

FIG. 7. Decay data from a cathode experiment at 6.21×10^{-3} A cm^{-2} ($i/i_L = 0.983$). —— slow decay; – – – – – fast decay ($\delta = 0.06$ cm); ● experimental $\bar{\Phi}_s$.

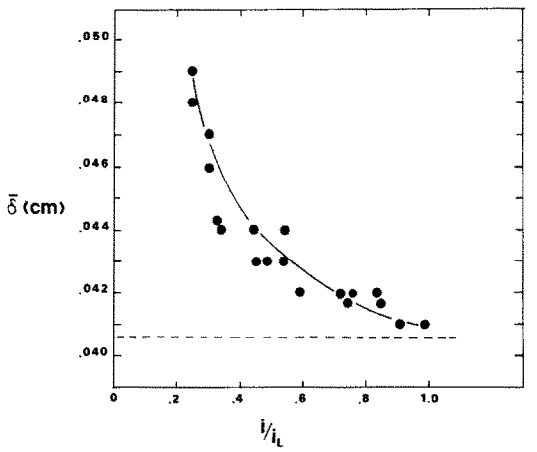

FIG. 8. Calculated boundary-layer thicknesses at different applied currents. ● experimental $\bar{\delta}$; — — — δ predicted from equation (1).

Fig. 8. Values of $\bar{\delta}$ decreased from 0.049 cm at $i/i_L = 0.25$ to 0.041 cm at $i/i_L = 0.98$. The trial and error values of $\bar{\eta}_0$ from duplicate decay experiments varied by at most 14%, and usually by less than 8%. Boundary-layer thicknesses from repeat experiments differed by less than 3%.

The analysis of the experimental data was based on the assumption that a single electrode reaction involving a single reacting species (Cu^{2+}) produced the experimental overpotential decay curves. When copper is electro-deposited from a $CuSO_4$–H_2SO_4 electrolyte without concomitant hydrogen gas evolution, the concentration of H^+ at the cathode surface will be greater than that in the bulk solution due to electric migration effects. Thus, there exists a H^+ ion contribution to the measured concentration overpotentials. The concentration increase in H^+ at a cathode during copper plating has been found from interferometric studies to be approximately equal to the

surface concentration decrease in Cu^{2+} [12]. As can be seen from the Nernst equation [equation (3)], however, concentration overpotentials due to reactant depletion at an electrode surface are much greater than those due to a surface concentration excess. Thus, from equation (3) and the concentration profiles in ref. [12], it can be concluded that the H^+ contribution to the measured concentration overpotentials is small.

To evaluate the curve fitting method of determining boundary-layer thicknesses, $\bar{\delta}$ values were compared with those obtained from existing correlations and theories. The Sherwood–Schmidt–Grashof number correlation, given by equation (1), was used to calculate $\bar{\delta}$ at $i/i_L = 1.0$. Physical property data for this and subsequent correlations and calculations are listed in Table 1. The derivation of equation (1) is based on an assumed linear variation of concentration throughout the entire boundary layer, i.e.

$$\frac{i}{n\mathcal{F}} = \frac{D(c_\infty - c_s)}{\delta_{eff}}. \tag{28}$$

δ_{eff}, defined as the effective boundary-layer thickness [22], is related to the true mass transport boundary-layer thickness (defined in equation (10)) by

$$\delta_{eff} = \tfrac{1}{2}\delta. \tag{29}$$

The value of δ_{eff}, as determined from the experimental limiting current (6.32×10^{-3} A cm^{-2}) and equation (28) (with $c_s = 0$), is 0.024 cm, hence $\bar{\delta} = 0.048$ cm. This boundary-layer thickness is $\sim 17\%$ larger than the value of 0.041 cm in Fig. 8 for $i/i_L \simeq 1.0$. The discrepancy in these $\bar{\delta}$ values cannot be explained at this time but may, in part, be due to the difficulty in accurately determining i_L from the galvanostatic polarization experiment and the $\pm 2.5\%$ error in the curve-fitted, boundary-layer thickness. The value of $\bar{\delta}$ calculated from equations (1) and (29) (0.0406 cm), on the other hand, agrees well with the present analysis.

Boundary-layer thicknesses below the limiting current were compared with those calculated from equation (2) and from the theoretical analysis of Ibl and Braun [4], who developed the following expression for δ,

$$\delta = \left(\frac{720\nu D^2\mathcal{F}}{\gamma g(\Lambda^2 - 4\Lambda + 5)}\right)^{1/5}\left(\frac{x}{i}\right)^{1/5} \tag{30}$$

where γ and Λ are defined as:

$$\gamma = \frac{\alpha_1}{n_1} - \frac{Z_2\alpha_2}{Z_2\Lambda^2(Z_2 - Z_3)} \tag{31}$$

$$\frac{1 - 4\Lambda + 5\Lambda^2}{2\Lambda^5} = \Gamma_2\left(1 - \frac{Z_2}{Z_3}\right). \tag{32}$$

In equations (31) and (32), Z_i is the ionic charge of species i, Γ_i is the transference number and α_i is the densification coefficient. $\delta(x)$ in equations (2) and (30) was integrated over an electrode of height L, to obtain an expression for the height-averaged boundary-layer thickness, $\bar{\delta}$.

As shown in Fig. 9, a plot of $-\ln \bar{\delta}$ vs $-\ln i/i_L$, the curve-fitted boundary-layer thicknesses agree well with the theory of Ibl and Braun but are approximately twice as large as those predicted by equation (2). Equation (2) was obtained by fitting interferometrically measured boundary-layer thicknesses to a generalized correlation equation for $10^5 < Gr^* < 10^{10}$. The discrepancies in Fig. 9 may be due to the fact that the modified Grashof numbers for the curve fitted values of $\bar{\delta}$ are $\sim 10^{13}$, which is beyond the range of equation (2). The slope of a least-squares straight line through

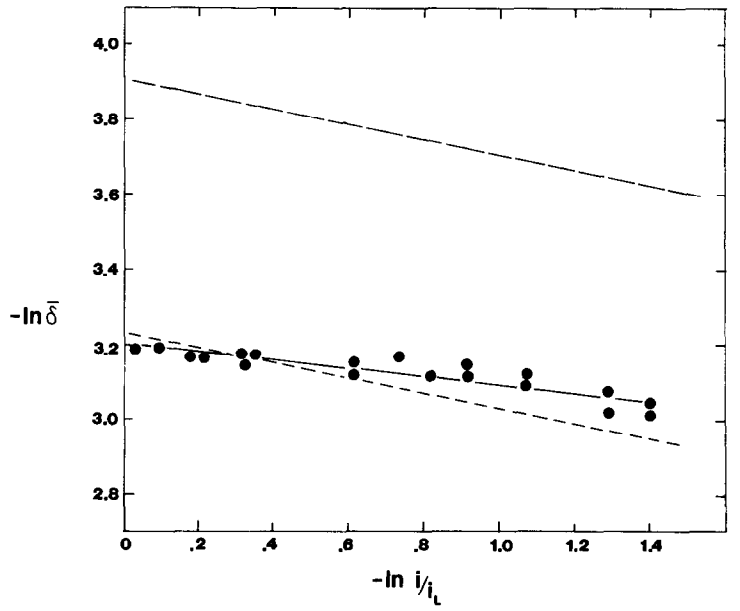

FIG. 9. Relationship between ln $\bar{\delta}$ and ln i/i_L. ● experimental $\bar{\delta}$; —— equation 2; – – – – equation (30).

the curve-fitted values of δ in Fig. 9 is -0.11, as opposed to a slope of -0.20 predicted from equations (2) and (30).

Although the results in Figs. 8 and 9 are encouraging, additional overpotential decay experiments are needed to verify the accuracy and applicability of the curve-fitting technique. The use of this method at low applied cathodic currents, in electrolytes of differing compositions and at cathodes of different lengths is currently being investigated and will be the subject of a future publication.

CONCLUSIONS

A non-contact electrochemical method of determining natural convection mass transfer boundary-layer thicknesses has been developed and tested. Concentration overpotentials after current interruption are converted, by use of the Nernst equation, to a dimensionless concentration fraction. The experimental data is then matched to a theoretical surface concentration decay model which was obtained by analyzing two limiting cases for transient natural convection mass transfer: (a) surface concentration changes by pure diffusion and (b) concentration changes by convection diffusion with constant velocities.

It was found in the mathematical analysis that the slow and fast decay extremes coincide exactly during the initial 10–20% change in surface concentration, thus permitting experimental overpotential data to be fitted to the theoretical model. In the region of coincidence the decay model is described by a simple analytical function. Mass transfer boundary-layer thicknesses were determined by equating the dimensionless time of the theoretical analysis and the real time of the experimental data. Calculated cathodic boundary-layer thicknesses decreased from 0.049 cm to 0.041 cm as the current density increased from $i/i_L = 0.25$ to $i/i_L = 0.98$. The boundary-layer thickness near the limiting current is in good agreement with $\bar{\delta}$ predicted from a Sherwood–Schmidt–Grashof number correlation. Curve-fitted boundary-layer thicknesses below the limiting current agree well with the theory of Ibl and Braun.

Acknowledgments—The author wishes to express his thanks to L. Nanis for his help in undertaking and pursuing this project.

REFERENCES

1. C. R. Wilke, M. Eisenberg and C. W. Tobias, Correlation of limiting currents under free convection conditions, *J. electrochem. Soc.* **100,** 513–523 (1953).
2. J. R. Selman and J. Newman, Free-convection mass transfer with a supporting electrolyte, *J. electrochem. Soc.* **118,** 1070–1078 (1971).
3. C. Wagner, The role of natural convection in electrolytic processes, *Trans. electrochem. Soc.* **95,** 161–173 (1949).
4. N. Ibl and U. Braun, Evaluation of the concentration changes near the electrodes in electrolysis with natural convection, *Chimia* **21,** 395–404 (1967).
5. N. Ibl and R. H. Muller, Studies of natural convection at vertical electrodes, *J. electrochem. Soc.* **105,** 346–353 (1958).
6. Y. Awakura, Y. Takenaka and Y. Kondo, Studies of the velocity profile in natural convection during copper deposition at vertical electrodes, *Electrochim. Acta* **21,** 789–797 (1976).
7. Y. Awakura and Y. Kondo, Concentration profile of $CuSO_4$ in the cathodic diffusion layer, *J. electrochem. Soc.* **123,** 1184–1192 (1976).
8. A. Tvarusko and L. W. Watkins, Laser interferometric study of the diffusion layer at a vertical cathode during non-steady-state conditions, *Electrochim. Acta* **14,** 1109–1118 (1969).
9. F. R. McLarnon, R. H. Muller and C. W. Tobias, Light-deflection errors in the interferometry of electrochemical mass transfer boundary layers, *J. Electrochem. Soc.* **122,** 59–64 (1975).
10. Y. Awakura, M. Okada and Y. Kondo, Profile of the refractive index in the cathodic diffusion layer of an electrolyte containing $CuSO_4$ and H_2SO_4, *J. Electrochem. Soc.* **124,** 1050–1057 (1977).
11. Y. Fakunaka, K. Denpo, M. Iwata, K. Maruoka and Y. Kondo, Concentration profile of Cu^{2+} ion near a plane vertical cathode in electrolytes containing $CuSO_4$ and an excess of H_2SO_4 as supporting electrolyte, *J. electrochem. Soc.* **130,** 2492–2500 (1983).
12. K. Denpo, T. Okumura, Y. Fukunaka and Y. Kondo, Measurement of concentration profiles of Cu^{2+} ion and H^+ ion near a plane vertical cathode by two-wavelength holographic interferometry, *J. electrochem. Soc.* **132,** 1145–1150 (1985).
13. Y. Fukunaka, M. Inuzuka, A. Tsuboi and Y. Kondo, Disappearance of cathodic boundary layer after interrupting the electrolytic current, *Denki Kagaku* **47,** 471–479 (1979).
14. Y. Fukunaka, T. Minegishi, N. Nishioka and Y. Kondo, Transient natural convection near a plane vertical electrode surface after reversing the electrolytic current, *J. electrochem. Soc.* **128,** 1274–1280 (1981).
15. Y. Fukunaka and Y. Kondo, Momentum and mass transfer in the transient natural convection along plane vertical electrode, *Electrochim. Acta* **26,** 1537–1546 (1981).
16. A. Brenner, A method of studying cathode films by freezing, *Proc. Am. Electropl. Soc.*, 95–98 (1940).
17. H. J. Read and A. K. Graham, Electrolyte films in acid copper plating baths, *Trans. electrochem. Soc.* **78,** 279–301 (1940).
18. L. Nanis, Evaluation of boundary layer thickness in electrolytic systems from decay of anodic concentration polarization, *Nature* **192,** 449–450 (1961).
19. I. R. Miller and L. Nanis, Effect of dissolved spreading solvent on monolayer pressure and water evaporation resistance. *Proc. 4th Int. Congress of Surface Active Substances*, Vol. 2, pp. 841–855. Gordon & Breach, New York (1967).
20. Y. Awakura, A. Ebata, M. Morita and Y. Kondo, The measurement of diffusivity of $CuSO_4$ in aqueous $CuSO_4$ and $CuSO_4$–H_2SO_4 solutions, *Denki Kagaku* **43,** 569–577 (1975).
21. Y. Awakura, A. Ebata and Y. Kondo, Distribution of local current densities during copper deposition on a plane vertical cathode, *J. electrochem. Soc.* **126,** 23–30 (1979).
22. C. W. Tobias, M. Eisenberg and C. R. Wilke, Diffusion and convection in electrolysis—a theoretical review, *J. electrochem. Soc.* **99,** 359C–365C (1952).

UNE METHODE ELECTROCHIMIQUE POUR DETERMINER LES EPAISSEURS DE COUCHE LIMITE EN CONVECTION NATURELLE MASSIQUE

Résumé—On développe une méthode électrochimique sans contact pour déterminer les épaisseurs de couche limite dans la convection naturelle massique. La décroissance variable de concentration après coupure du courant est éprouvée sur un modèle théorique de la concentration en surface. Les épaisseurs de couche limite sont déterminées en égalant le temps réel des données expérimentales et le temps de l'analyse théorique. La technique de correspondance des courbes est testée en réalisant une série d'expériences à la cathode plane verticale en cuivre, immergée dans une solution de 0,15 M $CuSO_4$. Il en résulte que les épaisseurs de couche limite décroissent depuis 0,049 à 0,041 cm quand on augmente le courant appliqué.

EIN ELEKTROCHEMISCHES VERFAHREN ZUR BESTIMMUNG DER GRENZSCHICHTDICKE BEI DER STOFFÜBERTRAGUNG DURCH NATÜRLICHE KONVEKTION

Zusammenfassung—Eine berührungslose elektrochemische Methode wurde entwickelt und erprobt, um die Grenzschichtdicke bei der Stoffübertragung durch natürliche Konvektion zu bestimmen. Zeitliche Ausgleichsvorgänge der Überkonzentration, die sich nach einer Unterbrechung der Stromzufuhr einstellen, wurden durch ein theoretisches Oberflächen–Konzentrationsmodell simuliert. Durch Gleichsetzen des Zeitmaßstabs der experimentellen Daten und des dimensionslosen Zeitmaßstabs der theoretischen Berechnungen wurde die Grenzschichtdicke ermittelt. Das Verfahren der Kurvenanpassung wurde anhand einer Reihe von Experimenten, welche an einer vertikalen ebenen Kupferkathode durchgeführt wurden, überprüft, bei denen eine 0,15 molare $CuSO_4$–1,85 molare H_2SO_4 Lösung als Elektrolytlösung verwendet wurde. Die Ergebnisse für die im Beharrungszustand ermittelte Grenzschichtdicke zeigen eine Abnahme von 0,049 auf 0,041 cm bei Zunahme des aufgeprägten Stromes.

ЭЛЕКТРОХИМИЧЕСКИЙ МЕТОД ОПРЕДЕЛЕНИЯ ТОЛЩИНЫ ПОГРАНИЧНОГО СЛОЯ ПРИ ЕСТЕСТВЕННОКОНВЕКТИВНОМ МАССОПЕРЕНОСЕ

Аннотация—Предложен и изучен беззондовый электрохимический метод определения толщины пограничного слоя при естественноконвективном массопереносе. Переходное изменение концентрации на поверхности электрода после отключения напряжения соответствовало теоретической модели. Толщины пограничного слоя находились из условия равенства промежутков времени, определенных из экспериментальных данных и теоретического анализа. Методика подбора формул для кривых исследовалась при проведении экспериментов по изменению концентрации на вертикально расположенном катоде, изготовленном из плоской медной пластины, погруженном в раствор 0,15 М $CuSO_4$–1,85 М H_2SO_4. Толщины установившегося пограничного слоя с увеличением силы подаваемого тока уменьшались от 0,049 до 0,041 см.